

A Graphical Representation of the Piezoresistance Coefficients in Silicon

YOZO KANDA

Abstract—The longitudinal and transverse piezoresistance coefficients, $\Pi(300\text{ K})$, at room temperature are plotted as a function of the crystal directions for orientations in the (100), (110), and (211) planes. The piezoresistance coefficients $\Pi(N, T)$, with an arbitrary impurity concentration N and at an arbitrary temperature T , are expressed by $\Pi(N, T) = P(N, T) \Pi(300\text{ K})$, where $P(N, T)$ is called the piezoresistance factor and is a function of the Fermi integral. The $P(N, T)$ is calculated by assuming that the simple power law dependence of the relaxation time on energy is valid. The graphs of $P(N, T)$ are plotted as functions of impurity concentration ranging from 10^{16} to 10^{20} cm^{-3} and temperature ranging from -75 to 175°C with a 25°C interval.

I. INTRODUCTION

SINCE C. S. SMITH [1] discovered the piezoresistance effect of semiconductors having anisotropic energy band structures, such as silicon and germanium, they have been widely used as stress and strain sensors. Recently, the knowledge of the piezoresistance effect has been required not only by sensor researchers but also by integrated-circuit designers and process engineers [2], [3].

The piezoresistance coefficients, usually required in an arbitrarily oriented coordinate system, can be calculated from a tensor transformation for the particular orientation. These calculations are long, laborious, and troublesome. Moreover, piezoresistance coefficients depend on impurity concentration and temperature.

This paper gives some of the typical piezoresistance coefficients of silicon as functions of crystal direction for common orientations, impurity concentrations, and temperatures. Many good review articles [4]–[7] have been published on the piezoresistance effect and its applications. This paper will complement these articles and should be of value to people designing piezoresistive sensors and integrated circuits.

II. DEPENDENCE ON CRYSTALLOGRAPHIC AXIS

According to the phenomenological description [6], piezoresistance, the fractional change in resistivity with small stress, is expressed by

$$\frac{\Delta\rho_\omega}{\rho} = \sum_{\lambda=1}^6 \pi_{\omega\lambda} X_\lambda \quad (1)$$

where X_λ is the component of the stress tensor in six-component vector notation and $\pi_{\omega\lambda}$ is the component of the piezoresistance tensor. In crystals with cubic symmetry, such as silicon and germanium, the tensor is given by

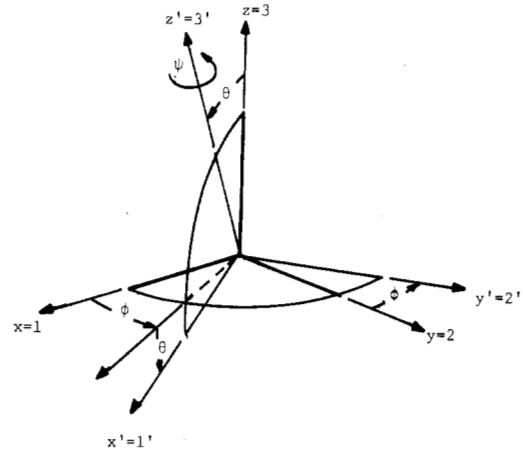


Fig. 1. Euler's angles.

$$[\pi_{\omega\lambda}] = \begin{bmatrix} \pi_{11} & \pi_{12} & \pi_{12} & 0 & 0 & 0 \\ \pi_{12} & \pi_{11} & \pi_{12} & 0 & 0 & 0 \\ \pi_{12} & \pi_{12} & \pi_{11} & 0 & 0 & 0 \\ 0 & 0 & 0 & \pi_{44} & 0 & 0 \\ 0 & 0 & 0 & 0 & \pi_{44} & 0 \\ 0 & 0 & 0 & 0 & 0 & \pi_{44} \end{bmatrix} \quad (2)$$

The transformation from the crystal axes, x_i , to a Cartesian system of arbitrary orientation x'_i , noting that subscripts 1, 2, 3, 4, 5, 6 correspond to 11, 22, 33, 23, 13, 12, respectively, can now be expressed

$$x'_i = \alpha_{ij} x_j$$

$$X'_\mu = X'_{ik} = \alpha_{ij} \alpha_{kl} X_{il} = \alpha_{ij} \alpha_{kl} X_\lambda$$

$$\pi_{ijk\mu} X_{km} = \begin{cases} \pi_{\lambda\mu} X_\mu, & \mu = 1, 2, 3 \\ \frac{1}{2} \pi_{\lambda\mu} X_\mu, & \mu = 4, 5, 6. \end{cases}$$

The transformation is given by direction cosines, between the two axes, which can be expressed in terms of Euler's angles (shown in Fig. 1) as follows, where $c\phi \equiv \cos \phi$, $s\psi \equiv \sin \psi$, etc.

$$\begin{bmatrix} l_1 & m_1 & n_1 \\ l_2 & m_2 & n_2 \\ l_3 & m_3 & n_3 \end{bmatrix} = \begin{bmatrix} c\phi c\theta c\psi - s\phi s\psi & s\phi c\theta c\psi + c\phi s\psi & -s\theta c\psi \\ -c\phi c\theta s\psi - s\phi c\psi & -s\phi c\theta s\psi + c\phi c\psi & s\theta s\psi \\ c\phi s\theta & s\phi s\theta & c\theta \end{bmatrix} \quad (3)$$

Here, two typical piezoresistance effects will be considered when uniaxial stress is applied in the material. One is a longitudinal piezoresistance coefficient when the current and field

Manuscript received April 28, 1981; revised September 1, 1981.

The author is with the Hamamatsu University School of Medicine, Hamamatsu, 431-31, Japan.

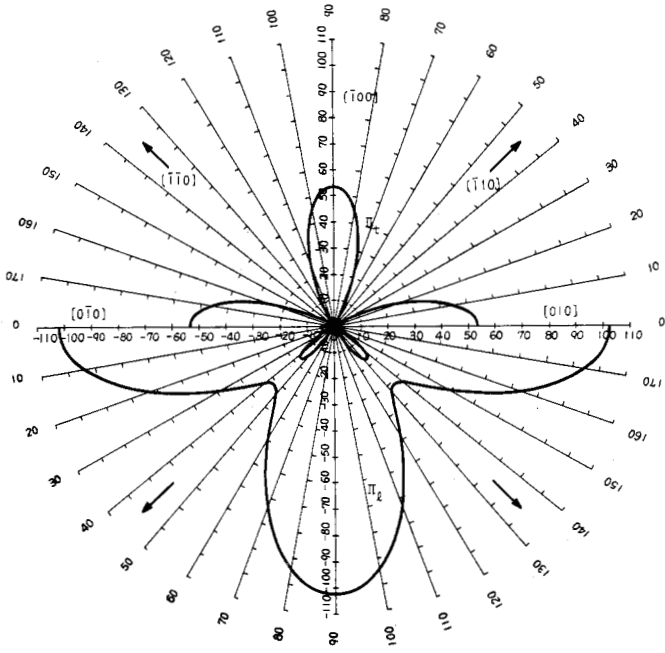


Fig. 2. Room temperature piezoresistance coefficients in the (001) plane of n-Si (10^{-12} cm²/dyne).

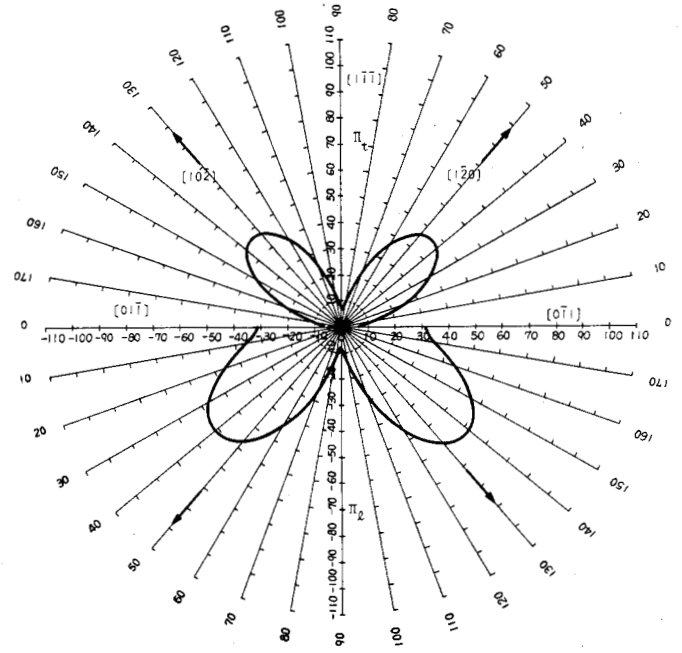


Fig. 4. Room temperature piezoresistance coefficients in the (211) plane of n-Si (10^{-12} cm²/dyne).

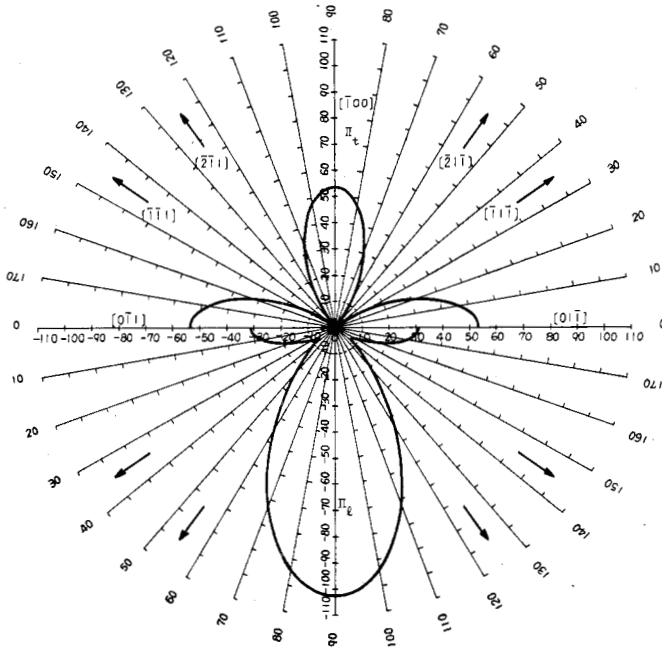


Fig. 3. Room temperature piezoresistance coefficients in the (011) plane of n-Si (10^{-12} cm²/dyne).

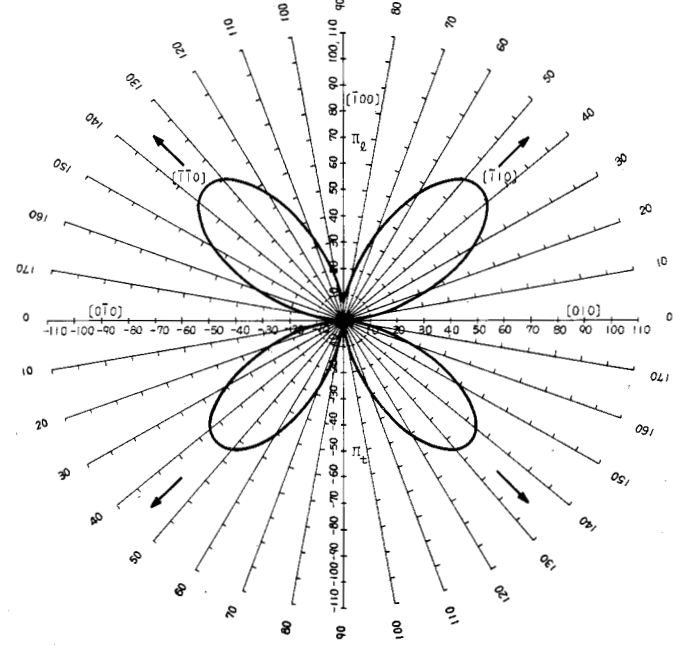


Fig. 5. Room temperature piezoresistance coefficients in the (001) plane of p-Si (10^{-12} cm²/dyne).

are in the direction of the stress noted by Π_l . The other is a transverse piezoresistance coefficient when the current and field are perpendicular to the stress noted by Π_t .

$$\pi'_{11} = \Pi_l = \pi_{11} - 2(\pi_{11} - \pi_{12} - \pi_{44})(l_1^2 m_1^2 + m_1^2 n_1^2 + n_1^2 l_1^2) \quad (4)$$

and

$$\pi'_{12} = \Pi_t = \pi_{12} + (\pi_{11} - \pi_{12} - \pi_{44})(l_1^2 l_2^2 + m_1^2 m_2^2 + n_1^2 n_2^2). \quad (5)$$

In an (lmn) plane, the graph can be obtained by making the axis $3'$ normal to the plane, that is,

$$[l_3 m_3 n_3] = (l^2 + m^2 + n^2)^{-1/2} [lmn]$$

and by rotating the angle ψ from zero to π . The graphs of room temperature Π_l and Π_t are plotted as a function of crystal direction for orientations in the (001), (011), and (211) planes and are shown in Figs. 2-7. The graphs of (111) planes are omitted because of circular symmetry to the origin. The graphs are shown in units of 10^{-12} cm²/dyne based on the data of Smith [1] (shown in Table I). The upper halves of

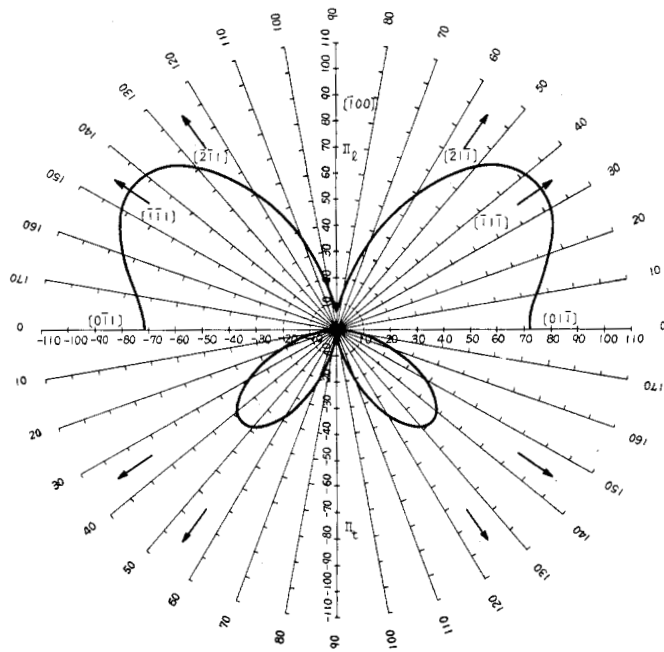


Fig. 6. Room temperature piezoresistance coefficients in the (011) plane of p-Si (10^{-12} cm²/dyne).

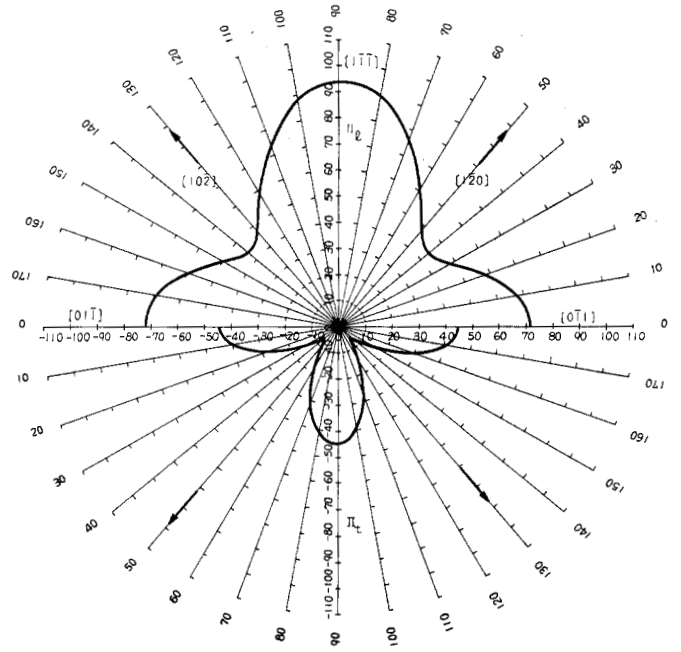


Fig. 7. Room temperature piezoresistance coefficients in the (211) plane of p-Si (10^{-12} cm²/dyne).

the graphs show positive values of the piezoresistance coefficients, that is, the resistivities increase with tensile stresses. The lower halves in the figures show negative values of the piezoresistance coefficients, that is, the resistivities decrease with tensile stresses.

III. DEPENDENCE ON IMPURITY CONCENTRATION AND TEMPERATURE

The conductivity tensor $\sigma_{\alpha\beta}$ is the sum of the conductivity $\sigma_{\alpha\beta}^i$ of the carriers near each extremum

$$\sigma_{\alpha\beta} = \sum_i \sigma_{\alpha\beta}^i. \quad (6)$$

The stress-induced change in conductivity is the sum of the stress-induced change in conductivity of the carriers near each extremum

$$\Delta\sigma_{\alpha\beta} = \sum_i \Delta\sigma_{\alpha\beta}^i. \quad (7)$$

Equation (1) may be rewritten by the conductivity

$$\frac{\Delta\sigma_{\alpha\beta}}{\sigma} = \frac{\Delta\sigma_{\omega}}{\sigma} = \sum_{\lambda} \Pi_{\omega\lambda} X_{\lambda} \quad (8)$$

where σ is the average conductivity.

The conductivity for each ellipsoid or for each species i of carrier in a degenerate band [7] is

$$\sigma_{\alpha\beta}^i = -e^2 \int \frac{\partial f_0}{\partial E} \tau_{\alpha\beta}^i v_{\alpha}^i v_{\beta}^i dK \quad (9)$$

where f_0 is the Fermi distribution function

$$f_0 = \frac{1}{1 + \exp(E_i - E_F/k_B T)}$$

and k_B is Boltzmann's constant. E_F is the Fermi energy, v_{α}^i is the group velocity of the carriers

$$\Delta v_{\alpha}^i = \frac{1}{h} \frac{\partial E_i}{\partial K_{\alpha}}$$

and $\tau_{\alpha\beta}^i$ is the relaxation time.

In order to make calculations feasible, it is assumed that the relaxation time is isotropic, depending only on energy

$$\Delta\tau_i = \frac{\partial \tau_i}{\partial E} \Delta E_i$$

and

$$\tau = \tau_0 E^s.$$

Transforming from variables K_i , K_j to the energy E_i and solid angle Ω , and noting the energy, (9) is rewritten as

$$\begin{aligned} \sigma &= \frac{-8\pi}{9} e^2 \int \frac{\partial f_0}{\partial E} \tau_i \frac{h^2}{m^2} K^4 dK \cdot \frac{9}{8\pi} \int \frac{K_i K_j}{K^2} d\Omega \\ &= \frac{-8\pi}{9} e^2 \psi'_{ij} \int \frac{\partial f_0}{\partial E} \cdot \tau \cdot E^{3/2} dE \cdot \frac{\sqrt{2m}}{h^3} \\ &= \frac{16\pi}{9} e^2 \frac{\sqrt{2m}}{h^3} \psi'_{ij} \int f_0 \frac{\partial}{\partial E} (\tau E^{3/2}) dE \\ &= \frac{16\pi}{9} e^2 \frac{\sqrt{2m}}{h^3} \psi'_{ij} \tau_0 \left(s + \frac{3}{2} \right) \int f_0 E^{s+(1/2)} dE \\ &= \frac{16\pi}{9} e^2 \frac{\sqrt{2m}}{h^3} \psi'_{ij} \tau_0 \left(s + \frac{3}{2} \right) (k_B T)^{s+(3/2)} \\ &\quad \cdot F_{s+(1/2)} \left(\frac{E_F}{k_B T} \right) \end{aligned} \quad (10)$$

where

TABLE I
PIEZORESISTANCE COMPONENTS AT ROOM TEMPERATURE IN UNITS OF
 $10^{-12} \text{ cm}^2/\text{dyne [1]}$

Material	n-Si	p-Si
$\rho (\Omega \cdot \text{cm})$	11.7	7.8
π_{11}	-102.2	+6.6
π_{12}	+53.4	-1.1
π_{44}	-13.6	+138.1

$$F_{s+(1/2)} \left(\frac{E_F}{k_B T} \right)$$

is the Fermi integral [8], defined by

$$\int_0^\infty \frac{E^{s+(1/2)}}{1 + \exp(E - E_F/k_B T)} dE = F_{s+(1/2)} \left(\frac{E_F}{k_B T} \right) \cdot (k_B T)^{s+(3/2)}.$$

The change in conductivity under stress is given by

$$\begin{aligned} \Delta\sigma_{\alpha\beta}^i &= -e^2 \int \Delta \left(\frac{\partial f_0}{\partial E} \tau v_i \cdot v_j \right) dK \\ &= -e^2 \left[\int \frac{\partial}{\partial E} \left(\frac{\partial f_0}{\partial E} \tau \right) v_i v_j \Delta E dK \right. \\ &\quad \left. + \int \frac{\partial f_0}{\partial E} \tau \frac{1}{h} \left(\frac{\partial \Delta E}{\partial k_i} v_j + \frac{\partial \Delta E}{\partial k_j} v_i \right) dK \right]. \end{aligned}$$

Integrating by parts, the second term of the above equation it is given by

$$\begin{aligned} \Delta\sigma_{\alpha\beta}^i &= e^2 \int \frac{\partial}{\partial E} \left(\frac{\partial f_0}{\partial E} \tau \right) v_i v_j \Delta E dK \\ &= \frac{16}{9} \pi e^2 \int_0^\infty \frac{\partial}{\partial E} \left(\frac{\partial f_0}{\partial E} \tau \right) EK^2 dK \cdot \frac{9}{8\pi} \frac{K_i K_j}{K^2} \Delta E d\Omega \\ &= \frac{16}{9} \pi e^2 \psi_{ij} \int_0^\infty \frac{\partial}{\partial E} \left(\frac{\partial f_0}{\partial E} \tau \right) E^{3/2} dE \cdot \frac{\sqrt{2m}}{h^3} \\ &= \frac{8\pi}{3} \pi e^2 \frac{\sqrt{2m}}{h^3} \psi_{ij} \int_0^\infty f_0 \frac{\partial}{\partial E} (\tau E^{1/2}) dE \\ &= \frac{8\pi}{3} e^2 \frac{\sqrt{2m}}{h^3} \tau_0 \left(s + \frac{1}{2} \right) \psi_{ij} \int_0^\infty f_0 E^{s-(1/2)} dE \\ &= \frac{8\pi}{3} e^2 \frac{\sqrt{2m}}{h^3} \tau_0 \psi_{ij} \left(s + \frac{1}{2} \right) (k_B T)^{s+(1/2)} \\ &\quad \cdot F_{s-(1/2)} \left(\frac{E_F}{k_B T} \right). \end{aligned} \quad (11)$$

From (6), (7), (10), and (11) we obtain

TABLE II
DENSITY-OF-STATES EFFECTIVE MASSES m_d/m AND SCATTERING
EXPONENTS S USED IN THE FERMI INTEGRAL CALCULATION

Materials	n-Si	p-Si
m_d/m ^{a)}	0.33	0.55
Number of Equivalent Valleys	6	
s	-1/2 ^{b)}	-1/2

^{a)}R. A. Smith [9].

^{b)}O. N. Tufte and E. L. Stelzer [10].

$$\begin{aligned} \frac{\Delta\sigma}{\sigma} &\sim \frac{1}{k_B T} \frac{1}{s + \frac{3}{2}} \frac{(s + \frac{1}{2}) F_{s-(1/2)} (E_F/k_B T)}{F_{s+(1/2)} (E_F/k_B T)} \\ &= \frac{1}{k_B T} \frac{1}{s + \frac{3}{2}} \frac{F'_{s+(1/2)} (E_F/k_B T)}{F_{s+(1/2)} (E_F/k_B T)} \end{aligned} \quad (12)$$

where a prime indicates derivative of the Fermi integral with respect to $E_F/k_B T$, and if $s = -\frac{1}{2}$

$$\begin{aligned} F_{s+(1/2)} (E_F/k_B T) &= \ln(1 + e^{E_F/k_B T}) \\ F'_{s+(1/2)} (E_F/k_B T) &= \frac{1}{1 + e^{-E_F/k_B T}}. \end{aligned}$$

Smith's data used in the calculation of the graphs in the previous section are in the range of Boltzmann distribution and were measured at 300 K. In this case, $f_0 = e^{(E - E_F)/k_B T}$ and (12) tends to

$$\frac{\Delta\sigma}{\sigma} \sim \frac{1}{k_B T} \frac{1}{s + \frac{3}{2}} \propto \Pi(300 \text{ K}). \quad (13)$$

Therefore, in general, the piezoresistance coefficient $\Pi(N, T)$ with an impurity concentration N and at a temperature T can be rewritten in the form

$$\Pi(N, T) = P(N, T) \cdot \Pi(300 \text{ K}) \quad (14)$$

where $P(N, T)$ is the piezoresistance factor and

$$P(N, T) = \frac{300}{T} \frac{F'_{s+(1/2)} (E_F/k_B T)}{F_{s+(1/2)} (E_F/k_B T)}. \quad (15)$$

The Fermi integral is the function of temperature and the Fermi energy. The Fermi energy is determined from N by using the following relation:

$$N = \nu \frac{\sqrt{2}}{\pi^2} \left(\frac{m_d^* k_B T}{h} \right)^{3/2} F_{1/2} (E_F/k_B T)$$

where m_d^* is the density-of-state effective mass and ν is the number of valleys. The graphs of $P(N, T)$ are calculated by using the data [9], [10] tabulated in Table II and are shown in Figs. 8 and 9.

According to Herring and Vogt [11], let us consider the physical aspect of the piezoresistance effect for a special case. The conduction ellipsoids lie on the $\langle 100 \rangle$ and equivalent

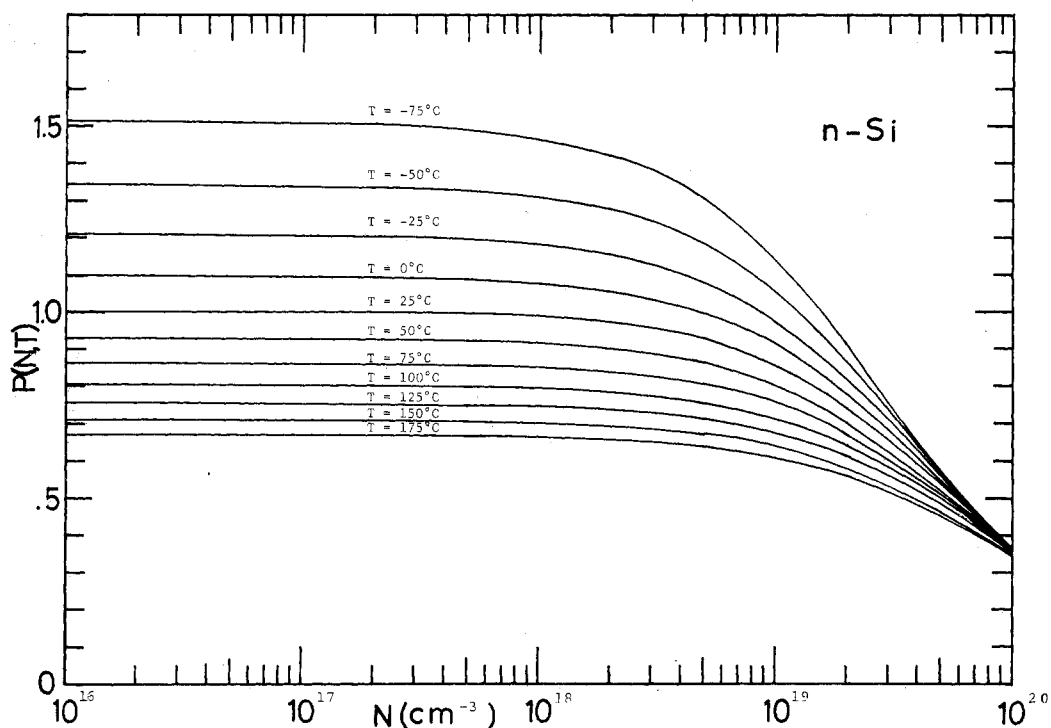


Fig. 8. Piezoresistance factor $P(N, T)$ as a function of impurity concentration and temperature for n-Si.

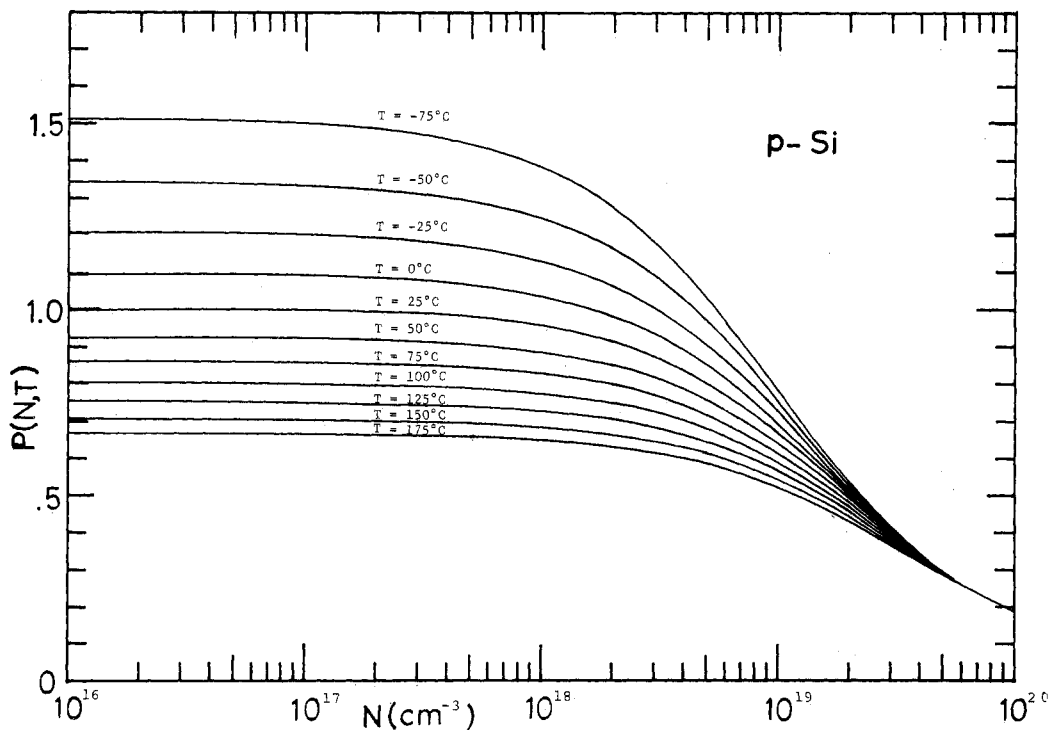


Fig. 9. Piezoresistance factor $P(N, T)$ as a function of impurity concentration and temperature for p-Si.

axes. The conductivity of an ellipsoid is

$$\sigma^i = n^i e \mu^i \quad (16)$$

where μ^i is the mobility, and n^i is the carrier concentration.

$$n^i = 2(2\pi m_d^* k_B T / h^2)^{3/2} e^{(E_F - E_i)/k_B T} \quad (17)$$

Assuming that μ^i is independent of stress, the change in the conductivity is

$$\Delta \sigma^i = \Delta n^i e \mu^i \quad (18)$$

It is given by

$$\Delta n^i = - \frac{n^i}{k_B T} (\Delta E^i - \Delta E_F) \quad (19)$$

Since the total number of electrons n is unchanged, we have

$$\Delta E_F = \frac{1}{\nu} \sum_i \Delta E^i \quad (20)$$

Equations (7), (18), (19), and (20) give [4], [7], [11]

$$\Delta \sigma = ne \left(\frac{-1}{k_B T} \right) \sum_i \mu^i \left(\Delta E^i - \frac{1}{\nu} \sum_i \Delta E^i \right) \quad (21)$$

The energy shift at the band-edge point of the i th ellipsoid for an arbitrary homogeneous strain is given by [11], [12]

$$\left. \begin{aligned} \Delta E^1(\langle 100 \rangle) &= \Delta E^4(\langle \bar{1}00 \rangle) = \Xi_d(\epsilon_{xx} + \epsilon_{yy} + \epsilon_{zz}) + \Xi_u \epsilon_{xx} \\ \Delta E^2(\langle 010 \rangle) &= \Delta E^5(\langle 0\bar{1}0 \rangle) = \Xi_d(\epsilon_{xx} + \epsilon_{yy} + \epsilon_{zz}) + \Xi_u \epsilon_{yy} \\ \Delta E^3(\langle 001 \rangle) &= \Delta E^6(\langle 00\bar{1} \rangle) = \Xi_d(\epsilon_{xx} + \epsilon_{yy} + \epsilon_{zz}) + \Xi_u \epsilon_{zz} \end{aligned} \right\} \quad (22)$$

where Ξ_d is the shift due to a dilation in the two directions normal to the ellipsoid axis, and Ξ_u is the shift due to a shear compounded of a stretch along the ellipsoid axis and a contraction in the two normal directions [11], $\epsilon_{\alpha\beta}$'s are the components of strain tensor. Now, consider the case when a uniaxial compressive stress X is applied in a [100] direction. The form for the strain components is expressed by [12]

$$[\epsilon_{\alpha\beta}] = \begin{bmatrix} s_{11} & s_{12} & s_{12} & 0 & 0 & 0 \\ s_{12} & s_{11} & s_{12} & 0 & 0 & 0 \\ s_{12} & s_{12} & s_{11} & 0 & 0 & 0 \\ 0 & 0 & 0 & \frac{1}{2}s_{44} & 0 & 0 \\ 0 & 0 & 0 & 0 & \frac{1}{2}s_{44} & 0 \\ 0 & 0 & 0 & 0 & 0 & \frac{1}{2}s_{44} \end{bmatrix} \begin{bmatrix} X \\ 0 \\ 0 \\ 0 \\ 0 \\ 0 \end{bmatrix} = \begin{bmatrix} s_{11} \\ s_{12} \\ s_{12} \\ 0 \\ 0 \\ 0 \end{bmatrix} \quad (23)$$

where the s_{ij} 's are the appropriate stiffness coefficients. We are considering π_{11} , that is, the current flows along [100] direction.

From (21), (22), and (23) we obtain

$$\Delta \sigma = ne \left(- \frac{1}{k_B T} \right) \Xi_u \frac{2}{3} (s_{11} - s_{12}) (\mu_{\parallel} - \mu_{\perp}) \quad (24)$$

Equations (6), (8), and (24) give

$$\begin{aligned} \frac{\Delta \sigma}{\sigma} &= \pi_{11} X = \frac{\left(- \frac{1}{k_B T} \right) \Xi_u \frac{2}{3} (s_{11} - s_{12}) (\mu_{\parallel} - \mu_{\perp})}{(\mu_{\parallel} + 2\mu_{\perp})} \\ &= \frac{2\Xi_u}{3k_B T} \frac{(s_{11} - s_{12})(L - 1)}{1 + 2L} \end{aligned} \quad (25)$$

where

$$L = \frac{\mu_{\perp}}{\mu_{\parallel}}$$

Similarly, we have

$$\begin{aligned} \pi_{12} &= \frac{\Xi_u}{3k_B T} \frac{(s_{11} - s_{12})(L - 1)}{1 + 2L} \\ \pi_{44} &= 0. \end{aligned} \quad (26)$$

We can get the relation between the phenomenological and the solid-state physical description from (4), (5), (14), (15), (25), and (26).

IV. DISCUSSION

The longitudinal and transverse piezoresistance coefficients at room temperature in the main crystal planes are given in Figs. 2-7. The relationship between the longitudinal piezoresistance coefficient Π_l and the strain gauge factor G will be considered, where G is normally used to characterize the strain sensor. G is defined as the fractional change in resistance $\Delta R/R_0$ per unit strain and is given by

$$G = (\Delta R/R_0)/\epsilon = 1 + 2\lambda + Y\Pi_l \quad (27)$$

where ϵ is the strain, λ is Poisson's ratio (the ratio of the magnitude of transverse strain to longitudinal strain resulting from the simple tension), and Y is Young's modulus. The first two terms represent the change in resistance due to dimensional changes while the last term represents the change in resistivity due to the strain. Fortunately, since the λ and Y in the crystal planes were calculated by Wortman and Evans [13], the G can be obtained.

The dependence of the piezoresistance coefficients on impurity concentration at a given temperature can be given by multiplying the piezoresistance factor $P(N, T)$, shown in Figs. 8 and 9, by the room temperature piezoresistance coefficient $\Pi(300 \text{ K})$. The values of the piezoresistance factor $P(N, T)$ were calculated by assuming that the scattering exponent $s = -\frac{1}{2}$ for n-Si and p-Si. This assumption gives good results in n-Si [10].

For p-type silicon, the calculated values of the $P(N, T)$ were compared quantitatively with the experimental values obtained by Mason *et al.* [14]. The deviations of the calculated values from the experimental ones are tabulated in Table III in terms of percent of the experimental value. Although the deviations are zero for the samples with concentration less than 10^{17} cm^{-3} , the deviations increase with increasing concentration; namely, about +12 percent for the sample with $N = 5 \times 10^{18} \text{ cm}^{-3}$, and about -20 percent for $N = 3 \times 10^{19} \text{ cm}^{-3}$. Since the scattering mechanism varies with impurity concentration and the scattering exponent S might not be uniquely determined over the wide impurity

TABLE III
THE DEVIATION OF CALCULATED PIEZORESISTANCE FACTOR $P(N,T)$
FROM THE EXPERIMENTAL ONE^a IN p-TYPE SILICON (PERCENTAGE)

concentration (cm^{-3}) temperature ($^{\circ}\text{C}$)	$<10^{17}$	5×10^{18}	3×10^{19}
	(%)	(%)	(%)
-50	0	+7	-24
0	0	+10	-23
25	0	+13	-21
50	0	+13	-20
100	0	+14	-19
150	0	+13	-9

^aW. P. Mason, J. J. Forst, and L. M. Tornillo [14].

concentration range, the calculated values deviate from the experimental ones with increasing impurity concentration. The scattering exponent $s = -\frac{1}{2}$ used in the calculation corresponds to the lattice scattering. More accurate calculation including various scattering mechanism remains as a future problem.

According to Tufte and Stelzer [15], the average piezoresistance coefficients of diffused layers will be only slightly larger than the piezoresistance coefficients in the uniformly doped material having an impurity concentration equal to the surface concentration of the diffused layer.

ACKNOWLEDGMENT

The author would like to thank T. Toyabe of the Hitachi Central Research Laboratory for discussions and support in the computer calculation, C. Gross of the NASA-Langley

Research Center, and T. Hara of Hosei University for discussions and J. Sugaya for typing. Help of T. Yamaguchi and K. Shogenji of Shizuoka University in calculation is also acknowledged.

REFERENCES

- [1] C. S. Smith, "Piezoresistance effect in germanium and silicon," *Phys. Rev.*, vol. 94, pp. 42-49, 1954.
- [2] Y. Kanda and M. Migitaka, "Effect of mechanical stress on the offset voltages of Hall devices in Si IC," *Phys. Status Solidi (a)*, vol. 35, pp. K115-K118, 1976.
- [3] —, "Design consideration for Hall device in Si IC," *Phys. Status Solidi (a)*, vol. 38, pp. K41-K44, 1976.
- [4] R. W. Keyes, "The effect of elastic deformation on the electrical conductivity of semiconductors," in *Solid State Physics*, vol. 11, F. Seitz and D. Turnbull, Eds. New York: Academic Press, 1960, pp. 149-221.
- [5] M. Dean and R. D. Douglas, Eds., *Semiconductor Strain Gauges*. New York: Academic Press, 1962.
- [6] R. N. Thurston, "Use of semiconductor transducers in measuring strain, accelerations, and displacements," in *Physical Acoustics*, vol. 1, pt. B. New York: Academic Press, 1964, pp. 215-235.
- [7] G. L. Bir and G. E. Pikus, *Symmetry and Strain-Induced Effects in Semiconductors*. New York: Wiley, 1974.
- [8] A. H. Wilson, *Theory of Metals*, 2nd ed. Cambridge, England: Cambridge Univ. Press, 1953, p. 147.
- [9] R. A. Smith, *Semiconductors*. Cambridge, England: Cambridge Univ. Press, 1959.
- [10] O. N. Tufte and E. L. Stelzer, "Piezoresistive properties of heavily doped n-type silicon," *Phys. Rev.*, vol. 133, pp. A1705-A1716, 1964.
- [11] C. Herring and E. Vogt, "Transport and deformation-potential theory for many-valley semiconductors with anisotropic scattering," *Phys. Rev.*, vol. 101, pp. 944-961, 1956.
- [12] Y. Kanda, "Effect of stress on germanium and silicon p-n junction," *Jap. J. Appl. Phys.*, vol. 6, pp. 475-485, 1967.
- [13] J. J. Wortman and R. A. Evans, "Young's modulus, shear modulus, and Poisson's ratio in silicon and germanium," *J. Appl. Phys.*, vol. 36, pp. 153-156, 1965.
- [14] W. P. Mason, J. J. Forst, and L. M. Tornillo, Instrument Society of America Conference Prepr. No. 15 NY60 (1960).
- [15] O. N. Tufte and E. L. Stelzer, "Piezoresistance properties of silicon diffused layers," *J. Appl. Phys.*, vol. 34, pp. 313-318, 1963.